HHS Public Access

Author manuscript

Stroke. Author manuscript; available in PMC 2016 July 01.

Published in final edited form as:

Stroke. 2015 July ; 46(7): 1956–1965. doi:10.1161/STROKEAHA.115.008939.

Inhibition of WNK3 kinase signaling reduces brain damage and accelerates neurological recovery after stroke

Gulnaz Begum, PhD[#], **Hui Yuan, PhD**[#], **Kristopher T. Kahle, MD, PhD**[##], **Liaoliao Li, PhD**, **Shaoxia Wang, PhD**, **Yejie Shi, MD, PhD**, **Boris E. Shmukler, PhD**, **Sung-Sen Yang, MD**, **Shih-Hua Lin, MD**, **Seth L. Alper, MD, PhD**, and **Dandan Sun, MD, PhD**[§]

Department of Neurology, University of Pittsburgh, Pittsburgh, PA, (G.B., H.Y., L.L., S.W., Y.S., D.S.); Department of Neurosurgery, Boston Children's Hospital and Harvard Medical School, Boston, MA (K.T.K.); Manton Center for Orphan Diseases, Harvard Medical School, MA (K.T.K.); Renal Division and Vascular Biology Center, Beth Israel Deaconess Medical Center, and Department of Medicine, Harvard Medical School, Boston, MA (B.E.S., S.L.A); Division of Nephrology, Dept. of Medicine, Tri-Service General Hospital, National Defense Medical Center, Taipei, Taiwan (SS.Y., SH.L); Veterans Affairs Pittsburgh Health Care System, Geriatric Research, Educational and Clinical Center, Pittsburgh, PA (D.S)

[#] These authors contributed equally to this work.

Abstract

BACKGROUND AND PURPOSE—WNK kinases, including WNK3, and the associated downstream SPAK and OSR1 kinases, comprise an important signaling cascade that regulates the cation-chloride cotransporters. Ischemia-induced stimulation of the bumetanide-sensitive Na^+-K^+-Cl^- cotransporter (NKCC1) plays an important role in the pathophysiology of experimental stroke, but the mechanism of its regulation in this context is unknown. Here, we investigated the WNK3-SPAK/OSR1 pathway as a regulator of NKCC1 stimulation and their collective role in ischemic brain damage.

METHOD—Wild-type *WNK3 (WT)* and *WNK3* knockout (KO) mice were subjected to ischemic stroke via transient middle cerebral artery (MCA) occlusion. Infarct volume, brain edema, blood brain barrier (BBB) damage, white matter demyelination, and neurological deficits were assessed. Total and phosphorylated forms of WNK3 and SPAK/OSR1 were assayed by immunobloting and immunostaining. *In vitro* ischemia studies in cultured neurons and immature oligodendrocytes were conducted using the oxygen-glucose deprivation/reoxygenation method.

RESULTS—WNK3 KO mice exhibited significantly decreased infarct volume and axonal demyelination, less cerebral edema, and accelerated neurobehavioral recovery compared to WNK3 WT mice subjected to MCA occlusion. The neuroprotective phenotypes conferred by WNK3 KO were associated with a decrease in stimulatory hyper-phosphorylations of the SPAK/OSR1 catalytic T-loop and of NKCC1 stimulatory sites Thr^{203}/Thr^{207}/Thr^{212}, as well as with decreased

[§]**Corresponding author:** Dandan Sun, M.D., Ph.D., University of Pittsburgh, Department of Neurology, S-598 South Biomedical Science Tower (BST), 3500 Terrance St., Pittsburgh, PA 15213, USA, sund@upmc.edu, Phone: (412) 624-0418, Fax: 412-648-3321.
[#]*Present affiliation:* Departments of Neurosurgery and Pediatrics, Yale University School of Medicine, New Haven, CT 06511, USA.

DISCLOSURES

None.

cell surface expression of NKCC1. Genetic inhibition of WNK3 or siRNA knockdown of SPAK/OSR1 increased the tolerance of cultured primary neurons and oligodendrocytes to *in vitro* ischemia.

CONCLUSION—These data identify a novel role for the WNK3-SPAK/OSR1-NKCC1 signaling pathway in ischemic neuroglial injury, and suggest the WNK3-SPAK/OSR1 kinase pathway as a therapeutic target for neuroprotection following ischemic stroke.

Keywords

Bumetanide; cation-chloride cotransporters; ischemic stroke; KCC2; neuroprotection; NKCC1; OSR1; SPAK; WNK1; WNK3

INTRODUCTION

Ischemic stroke is a common disease with high morbidity and mortality. Impaired cellular ion homeostasis causes ischemic neuroglial death [1]. Glutamate-stimulated, N-methyl-D-aspartate receptor ($NMDA_R$)-dependent perturbation of Na^+ and Ca^{2+} homeostasis is a well-known contributor to ischemia-induced brain damage[1] , but targeting of this pathway has limited neuroprotective efficacy in humans [2]. Derangements in other NMDA-independent ion transport pathways also contribute to ischemic brain damage [3, 4]. Genetic or pharmacological blockade of voltage-gated K^+ channels [5], of the acid-sensing ion channel 1a (ASIC1a) [3], and of the SUR1 (sulfonylurea receptor 1)-TRPM4 (transient receptor potential melastatin 4) channel complex [6] have also been shown to be neuroprotective, suggesting their potential as novel therapeutic targets.

Ischemia-induced stimulation of the bumetanide-sensitive Na^+-K^+-Cl^- cotransporter (NKCC1) has been demonstrated to play an important role in the pathophysiology of experimental stroke, leading to cellular Na^+ overload, cytotoxic edema, and necrotic and apoptotic cell death [7, 8]. However, the molecular mechanisms underlying NKCC1 activation in ischemic stroke are not known. The Cl^--sensing WNK (with no lysine) and the SPAK/OSR1 (Ste20/SPS1-related proline-alanine-rich protein kinase / oxidative stress-responsive 1) serine-threonine kinases comprise an evolutionarily conserved signaling pathway that regulates the activities of NKCC1 and multiple other ion transporters and channels to control cell volume and epithelial ion transport [9-13]. WNK kinases, including WNK3, associate with and activate SPAK/OSR1 by phosphorylation of its T-loop at Thr^{233} and Thr^{185}. Activated SPAK/OSR1, in turn, stimulates NKCC1 activity by directly phosphorylating NKCC1 at multiple N-terminal threonines (Thr), including Thr^{203}/Thr^{207}/Thr^{212} [10]. The role of WNK-SPAK/OSR1 signaling in regulation of the related thiazide-sensitive NCC and furosemide-sensitive NKCC2 cotransporters during renal epithelial NaCl and K^+ homeostasis has been well characterized [14, 15]. However, the function of WNK-SPAK/OSR1 signaling in the brain is essentially unknown.

WNK3 is a particularly compelling candidate regulatory kinase of NKCC1, given its abundant expression in brain [16-18], its physical association with NKCC1 [19], and the potent inhibitory effect of catalytically-inactive WNK3 on NKCC1 *in vitro* [17, 20, 21]. We hypothesized that inhibition of WNK-SPAK/OSR1 signaling might prevent the

phosphorylation required for NKCC1 activation and thereby reduce NKCC1-dependent cerebral injury following ischemic stroke. Our experimental approach incorporated genetic knockdown of each component of the WNK3-SPAK/OSR1 pathway in *in vitro* and *in vivo* models of ischemia. We found inhibition of WNK3-SPAK/OSR1-dependent signaling protects neurons and oligodendrocytes against injury and death by reducing ischemia-induced phospho-activation and membrane expression of NKCC1.

METHODS

Animals

WNK3 (C57Bl/6J) transgenic and NKCC1 (SV129/Black swiss) transgenic mice were housed in a temperature-controlled room on a 12-hour light/12-hour dark cycle with standard mouse diet and water ad libitum. The mice were used for study at ages 2-3 months. All studies were in compliance with the guidelines outlined in the Guide for the Care and Use of Laboratory Animals from the U.S. Department of Health and Human Services and were approved by the University of Pittsburgh Medical Center Institutional Animal Care and Use Committee.

Genetic analysis of *WNK3* insertional knockout (*WNK3* KO) mice

Female *WNK3*$^{-/-}$ and male *WNK3*$^{Y/-}$ knockout mice were generated from the ES cell line *RRJ530* (Bay Genomics) by the Mutant Mouse Regional Resource Centers at the University of California-Davis (mmrrc.ucdavis.edu), as described in the online-only Data Supplement. Immunoblot analysis with a specific anti-WNK3 antibody [22] confirmed the absence of WNK3 protein in the brain of *WNK3* KO mice (**Figure I** online-only Data Supplement). WNK3 KO mice exhibited normal phenotypes, which are consistent with previous reports on the normal electrolyte balance and grossly normal phenotypes of unstressed *WNK3* KO mice [23, 24].

Sequencing of mouse *WNK3* cDNA

Mouse *WNK3* cDNA from brain and kidney was PCR-amplified as overlapping cDNA fragments, purified from 1% agarose gel and sequenced. Tissue distribution of *WNK3* transcripts (**Figure I A, B** online-only Data Supplement**)** and genotyping of WNK3 KO mice are described in the Supplemental Materials & Methods.

Middle cerebral artery occlusion (MCAO) and reperfusion

Adult *WNK3* WT (female *WNK*$^{+/+}$ and male *WNK*$^{Y/+}$), adult *WNK3* KO (female *WNK3*$^{-/-}$ and male *WNK3*$^{Y/-}$), and adult male *NKCC1* WT or KO mice (*NKCC1*$^{+/+}$ and *NKCC1*$^{-/-}$ mice, originally developed by Flagella et al., [25], each weighing approximately 25–30 g at the ages of 2-3 months, were used in this study. Focal cerebral ischemia was induced by 60-min middle cerebral artery (MCA) occlusion, as previously described [26] and detailed description is provided in the online-only Data Supplement.

Neurological function analysis

Sensorimotor neurological deficit after surgery was evaluated in each mouse by a validated neurological function deficit scoring analysis as described in detail by Belayev et al.[27], according to the following scale: 0 = no observable deficit; 1 = forelimb flexion; 2 = forelimb flexion and decreased resistance to lateral push; 3 = forelimb flexion, decreased resistance to lateral push and unilateral circling; and 4 = forelimb flexion and impaired or absent ambulation.

Brain infarction volume and cerebral edema measurements

At 24 h reperfusion, mice were anesthetized with 5% halothane and then decapitated as described [28]. Coronal brain tissue slices (2 mm) were stained for 15 min at 37°C with 2% 2, 3, 5-triphenyltetrazolium chloride monohydrate (TTC, Sigma, St Louis, MO, USA) in PBS solution. Infarction volume was calculated as described [28]. The extent of hemispheric swelling was calculated using the equation: volume of ipsilateral hemisphere - volume of contralateral hemisphere)/volume of contralateral hemisphere. In addition, in a different cohort of mice, brain edema was determined by brain water content measurement as described previously [29].

Briefly, the ipsilateral and contralateral hemispheres were dissected and the wet weight of the tissue was measured. The tissue was dried at 120°C for 24 hrs. The hemispheric water content was calculated as the difference between wet and dry weights and expressed as a percentage of wet weight.

Primary cortical neuron cultures

Embryonic day 14-16 pregnant mice were anesthetized with 5% isoflurane and euthanized as described previously [8]. Fetuses were removed and the cortices dissected in ice-cold HBSS. The tissues were treated with 0.5 mg/ml trypsin at 37°C for 25 min. The cells were centrifuged at 350 g at 4°C for 4 min. The cells (200–1000 cells/mm^2) were cultured in plates or on glass coverslips coated with poly-D-lysine cultured in neurobasal medium containing B-27 supplements, GlutaMAX and penicillin/streptomycin (100 units/ml and 0.1 mg/ml, respectively) as described [8]. Cultures were incubated at 37°C in an incubator with 5% CO_2 and atmospheric air and re-fed with fresh medium every 3 days. Neurons in culture for 7-10 days (DIV 7-10) were used in the study.

Primary oligodendrocyte precursor cell (OPC) cultures

Neurospheres were prepared from E14.5 fetuses of timed pregnant female mice as described [30]. The dissociated cells were cultured in 25 cm^2 plastic culture flasks (2 brains/flask) in DMEM/F12 and 2% B27 neuronal supplement (Gibco, Baltimore, MD) plus 10 ng/mL EGF (Sigma, St. Louis, MO). The detailed procedures were described in the online-only Data Supplement.

Oxygen-glucose deprivation/reoxygenation (OGD/REOX) and cell death assay

OPCs or neurons grown in 6-well plates were rinsed with an isotonic OGD solution (pH 7.4) as described [31]. Cells were incubated in 0.5 ml of the OGD solution for 2 h in a hypoxic

incubator (model 3130 from Thermo Forma, Marietta, OH) containing 94% N_2, 1% O_2, and 5% CO_2 [31]. For reoxygenation, the cells were incubated for 1, 3, 6, or 24 h in the culture medium at 37°C in the incubator with 5% CO_2 and atmospheric air. Cell viability was assessed by propidium iodide (PI) uptake and retention of calcein-AM as described [31] and in the online-only Data Supplement.

siRNA treatment

Knockdown of SPAK or OSR1 protein expression in primary cortical neurons and OPCs was induced by the double-strand small interfering RNAs (siRNAs). Scramble siRNA (Silencer® Negative Control No. 1 siRNA, Cat. No. 12935-200) and siRNAs targeting mouse *SPAK* (ID: s79174) and *OSR1* (ID: s99266) were from Invitrogen. Scramble siRNA was used as control. Lipofectamine® RNAiMAX/siRNA complexes were formed in serum-free Opti-MEM® at 25°C for 5 min according to manufacturer's protocol. 250 μL of complexes was added into each well of 6-well plates. Studies were performed in cultures after 72 h transfection. siRNA-mediated knockdown of SPAK or OSR1 protein expression was validated by immunoblotting (**Figure II** online-only Data Supplement.).

Immunostaining and binary image analysis

Mice were anesthetized and transcardially-perfused as previously described [32]. Sections (−0.38 mm bregma, 35 μm) were incubated with blocking solution containing either rabbit anti-p-SPAK/p-OSR1 (1:50), sheep anti-pNKCC1 antibody (1:100), mouse anti-GFAP (1:100), mouse anti-APC (1:100), or mouse anti-MAP-2 (1:100). After rinsing with TBS for 30 min, sections were incubated with the following secondary antibodies (1:200): goat anti-rabbit Alexa Fluor 488-conjugated IgG and goat anti- mouse Alexa Flour 546-conjugated IgG; or donkey anti-sheep Alexa Fluor 488-conjugated IgG and donkey anti-mouse Alexa Fluor 546-conjugated IgG. Sections were incubated with nuclear stain TO-PRO-3 iodide (1:1000 in blocking solution) and mounted with Vectashield (Vector Laboratories, Burlingame, CA, USA). For negative controls, brain sections were stained with secondary antibody only. The imaging method and the binary image analysis are further described in the online-only Data Supplement Methods.

Luxol fast blue staining

White matter injury was quantified as previously reported [33] and is described in greater detail in the online-only Data Supplement.

The blood brain barrier (BBB) leakage measurement

To measure the BBB leakage, albumin infiltration in ischemic brains was examined by immunostaining as described previously [34]. Briefly, coronal sections were immunostained with albumin antibody (1:200), followed by incubation with goat anti- rabbit Alexa Fluor 488-conjugated IgG. Three to five consecutive images were acquired from each hemisphere from each brain section (n = 5 brains), using the confocal laser scanning microscope. Albumin signal intensity was measured with a frame size of 1024X1024 pixels. Quantification was done using Image J software. Background intensity in each original

image was subtracted and mean fluorescence intensity was obtained. The resulting values were then averaged and subjected to statistical analysis.

Biotinylation, membrane isolation, and immunoblotting

Cultured cells and brain cortex homogenates were prepared as previously described [35]. Biotinylation was as described in online-only Data Supplement.

Statistics

A total of 61 mice were used in the study, and no results were excluded from the analysis. All measurements were performed by investigators who were blinded to the experimental conditions. The number of animals studied was 80% powered to detect 20% changes with α (two-sided) = 0.05. Data were expressed as mean ± SD or SEM (as indicated). Statistical significance was determined by student's t-test, or one-way ANOVA using the Student-Newman-Keuls post-hoc test in case of multiple comparisons (SigmaPlot, Systat Software, Point Richmond, CA, USA). Repeated measures and paired t-tests were performed for immunostaining analysis in ischemic brains. Neuroscore was analyzed by the non-parametric Mann-Whitney test. A probability value < 0.05 was considered statistically significant.

RESULTS

Germline deletion of *WNK3* decreases infarct volume and demyelination and improves neurological recovery following ischemic stroke

Regional cerebral blood flow (rCBF) and gross neurovascular anatomy were indistinguishable in *WNK3* KO (female, male) and *WNK3* WT littermates (female, male) prior to, during, and after MCAO (**Fig. 1A**). However, after 24 h reperfusion (Rp) post-MCAO, *WNK3* KO brains exhibited a marked reduction (> 50%) in cortical infarct volume (38.2 ± 4.2 mm^3) relative to *WNK3* WT brains (79.4 ± 18.0 mm^3, $p < 0.05$, **Fig. 1A**). 8 WNK3 WT mice (4F/4M) and 8 WNK3 KO mice (4F/4M) were assessed in the evaluation of ischemic infarct volume. Smaller infarctions were also noted repeatedly at 3 days post-MCAO in *WNK3* KO brains by MRI (data not shown), ruling out the concern that the reduced infarct volume in *WNK3* KO mice at 24 h post-MCAO reflects a delayed development of post-ischemic damage of unreduced extent.

WNK3 KO brains also exhibited significantly less demyelination of external capsule (EC) white matter axonal tracks at day 3 Rp relative to WT *WNK3* brains (**Fig. 1B**, $p < 0.05$). Myelination was preserved in axonal bundles of the IL striatum of *WNK3* KO mice compared to *WNK3* WT mice (**Fig. 1B**). Importantly, the decreases in ischemic grey and white matter damage accompanying WNK3 deletion had functional consequences, as WNK3 KO mice exhibited accelerated neurological recovery following MCAO as compared to their WT littermates (**Fig. 1C**). All male mice (9 WNK3 WT, 8 WNK3 KO) were included in the analysis of neurological functional deficits in **Fig. 1 C**. The sensorimotor function of *WNK3* KO mice at days 3-7 Rp scored significantly better [27] than that of *WNK3* WT mice (**Fig. 1C**; n=10, $p < 0.05$). As shown in **Fig. 1D**, p-NKCC1 abundance in plasmalemmal membrane fractions was significantly elevated in the IL hemispheres of

WNK3 WT mice at 24 h Rp. In contrast, little change in p-NKCC1 was observed in the corresponding membrane or cytosol fractions from WNK3 KO brains. Similar phenotypes of reduced neurological deficits and preserved axonal myelination were detected in NKCC1$^{-/-}$ mice and in NKCC1 WT mice treated with NKCC1 inhibitor bumetanide (**Figure III** online-only Data Supplement).

WNK3 KO mice exhibit less cerebral edema and leakage across the blood brain barrier after ischemic stroke

We examined brain water content in a different cohort of *WNK3* WT and *WNK3* KO mice after ischemic stroke (see Methods for details). *WNK3* KO mice exhibited significantly less cerebral edema at 24 h after focal ischemia, compared to *WNK3* WT mice (**Fig. 2A**). Similar findings were obtained from measurement of the percentage of hemisphere swelling from the TTC-stained brain sections shown in **Fig.1A.** In addition, we evaluated the blood brain barrier (BBB) integrity by analyzing infiltration of blood albumin in the ischemic brain tissues. BBB integrity was compromised in *WNK3* WT mice at 3 days after focal ischemia, as reflected by a dramatic increase in albumin accumulation in ischemic brain tissues (**Fig. 2B, C,** arrows). In contrast, *WNK3* KO brains exhibited significantly less albumin infiltration (**Fig. 2B, C).** These data show WNK3 knockout reduces cerebral edema and the BBB breakdown after ischemic stroke.

Focal cerebral ischemia stimulates the activating phosphorylation of NKCC1 by the WNK and SPAK/OSR1 kinases

We next investigated activation of SPAK/OSR1-NKCC1 signaling in ischemic brains utilizing antibodies that recognize only the phosphorylated (i.e., active) species of SPAK/OSR1 (SPAK/OSR1 [T-loop] phospho-Thr^{233}/Thr^{185}) [36, 37] and of NKCC1 (phospho-Thr^{203}, Thr^{207}, and Thr^{212}) [38]. A marked elevation of p-SPAK/p-OSR1 (arrows, **Fig. 3A, B)** and p-NKCC1 (arrows, **Fig. 4A, B**) in ipsilateral (IL) peri-infarct areas (cortex and striatum) was detected at 6 h or 24 h Rp relative to the control contralateral (CL) cortex and striatum. The binary image analysis of the immnunofluorescence images separated specific immunological signal from background (**Figure IV A, B** online-only Data Supplement**)** in each image (**Fig. 3 and Fig. 4, A, B**). p-SPAK/p-OSR1 and p-NKCC1 immunoreactive signals were localized in neurons which are stained positively for the neuronal marker protein MAP2 (microtubule-associated protein-2) (double-arrowhead, **Fig. 3 and Fig. 4 A, B**). Expression of p-SPAK/p-OSR1 in total cells (TO-PRO 3^{+}) or neurons (MAP2^{+}) was further quantified (**Fig. 3**). However, p-SPAK/p-OSR1 was not detected in GFAP^{+} cells (astrocytes) of IL cortex or striatum at 6 h Rp (**Figure IV C** online-only Data Supplement), consistent with the delayed development of astrogliosis, usually beyond 48 h Rp [32].

In addition, expression of p-SPAK/p-OSR1 in the white matter of corpus callosum progressed from low levels at 6 h Rp (**Figure V** online-only Data Supplement), through increased level at 24 h Rp, to peak levels at 72 h Rp, returning to basal levels by day 7 (168 h Rp). The cells with robust expression of p-SPAK/p-OSR1 at 72 h Rp were confirmed as APC^{+} mature oligodendrocytes (**Fig. 3C**). These findings suggest that stimulation of the SPAK/OSR1 signaling pathway in ischemic brains was differentially regulated with regard to brain region and cell type. The delayed increase of p-SPAK/p-OSR1 and p-NKCC1 in the

IL corpus callosum white matter (arrows, **Fig. 3C, 4C**) is consistent with the timing of oligodendrocyte degeneration after MCAO [39]. Strikingly, knockout of *WNK3 in vivo* abrogated the ischemia-induced increases p-SPAK/p-OSR1 and p-NKCC1 in the cortex and striatum (**Fig. 3, 4**). In addition, abundance of p-SPAK/p-OSR1 and p-NKCC1 was decreased in the corpus callosum of APC^+ cells in WNK3 KO mice (**Fig. 3C, 4C**). In WNK3 KO white matter tissues, p-SPAK/p-OSR1-immunoreactive signals and p-NKCC1 signals (especially in the cytosol) remain detectable (**Fig. 3C and 4C**). A possible role for WNK1 or other WNKs in maintaining the residual NKCC1 phosphorylation in WNK3 KO brains remains to be tested.

Knockdown of WNK3 or SPAK/OSR1 protects neurons and OPCs against ischemic damage in culture

Robust SPAK/OSR1-NKCC1 phospho-activation was also confirmed in neurons or oligodendroglial precursor cell cultures (OPCs) in a model of *in vitro* ischemia (2 h oxygen and glucose deprivation [OGD] plus 24 h reoxygenation [REOX]). Activating phosphorylation of SPAK/OSR1 at 1-6 h REOX and surface expression of p-NKCC1 at 24 h REOX were detected in *WNK3* WT but not in *WNK3* KO neurons (**Fig. 5A, B**), and were accompanied by > 40% cell death in *WNK3* WT neurons (**Fig. 5C**). NKCC1 inhibition with bumetanide (BMT, 10 μM, 24 h) significantly reduced ischemic cell death of neurons and OPCs (**Fig. 5C, D**). Deletion of *WNK* or siRNA knockdown of *SPAK* or *OSR1* (**Figure II** online-only Data Supplement.) increased tolerance to OGD/REOX in neurons and OPCs (**Fig. 5C, D**). Indeed, no ischemic cell death was evident in untreated *WNK3* KO neurons or in WT neurons treated with *SPAK/OSR1* siRNAs (**Fig. 5C, D**). Significant protection was also detected in WT OPCs treated with *SPAK/OSR1* siRNAs. Additional studies are needed to determine the cell protection mechanisms (anti-apoptotic, anti-necrotic, or others).

DISCUSSION

The evolutionarily-conserved WNK-SPAK/OSR1 kinase signaling pathway maintains ionic homeostasis via the regulated phosphorylation of the cation-chloride cotransporters. Mutations of WNK1/WNK4 cause a Mendelian form of salt-sensitive human hypertension due to SPAK/OSR1-mediated hyper-phosphorylation and activation of renal NCC [14, 15]. However, the functions of the WNK-SPAK/OSR1 pathway in other tissues, including the brain, have been little studied. We now provide *in vitro* and *in vivo* evidence demonstrating that activation of the WNK3-SPAK/OSR1 kinase signaling pathway is associated with the pathophysiology of neuronal and oligodendrocyte injury following ischemic stroke. In particular, genetic inactivation of WNK3 or siRNA-mediated knockdown of SPAK/OSR1 prevented demyelination and reduced OPC death. Since white matter comprises half of human forebrain volume and is highly susceptible to ischemic damage [40], our data highlight the WNK/SPAK/NKCC1 signaling complex as a novel, potential therapeutic target for neuroprotection and preservation of myelination following stroke. Our current study suggests that WNK3-dependent SPAK/OSR1 phosphorylation of NKCC1 at $T^{203}/T^{207}/T^{212}$, a key N-terminal cytosplamic domain regulatory motif of the cotransporter, is required for ischemia-induced activation of NKCC1, at least in part via effects on transporter surface expression [22, 38]. These findings are consistent with the reported roles of the WNK-SPAK/

OSR1 kinase cascade in plasmalemmal accumulation of ion transporters through their decreased ubiquitination and lysosomal degradation [41, 42].

Previous reports revealed that increased NKCC1 function contributes to ischemic brain damage by cellular influx of Na^+ and Cl^- and, secondarily, of Ca^{2+}, triggering cell swelling, breakdown of the blood brain barrier [43], and damage to the endoplasmic reticulum and mitochondria that leads to both necrotic and apoptotic cell death [44-46]. How ischemia activates the WNK3-SPAK/OSR1-NKCC1 signaling cascade remains unclear. Recent studies by Piala et al revealed WNK1 as a direct Cl^- sensor, with Cl^- binding at the active site and leading to Cl^--dependent inhibition of WNK1 autophosphorylation [13]. Increased tissue osmolality, or pathological changes in ionic contents, such as Cl^-, may catalyze dysregulated WNK-SPAK/OSR1 activity by direct interaction with the WNK catalytic site [47-49]. Alternatively, inflammation may play a role in WNK-SPAK/OSR1 activation. Indeed, pro-inflammatory cytokine tumor necrosis factor-α (TNF-α) stimulated colonic SPAK expression and activation during the pathogenesis of intestinal inflammation [50], and oxidative stress mediated by H_2O_2 or NH_4Cl triggered NKCC1 phosphorylation and astrocyte swelling [51]. An increase in $[Ca^{2+}]_i$ via activation of ionotropic or metabotropic glutamate receptors was also shown to increase NKCC1 activity in neurons [52, 53]. All these factors are present and active in the ischemic brain, and future studies will be necessary to elucidate their possible roles in activation of the WNK3-SPAK/OSR1-NKCC1 cascade.

Taken together, our findings on the WNK3-dependence of SPAK/OSR1-NKCC1 phospho-activation in ischemic stroke are compelling in the context of novel pharmacotherapeutic strategies. Inhibition of the widely expressed SPAK/OSR1 or NKCC1 might be expected to elicit effects outside the CNS, as reflected by the extra-CNS phenotypes of their KO mice [e.g., see [11, 54]]. In contrast, the abundant expression of WNK3 in brain [17, 18, 20, 55, 56] and the normal electrolyte balance and grossly normal phenotypes of unstressed *WNK3* KO mice [23, 24] suggest that WNK3 inhibition might modulate brain SPAK/OSR1 and NKCC1, reducing gray and white matter damage and improving neurological recovery following ischemic stroke, with minimal effects on other organ systems including the kidney.

Supplementary Material

Refer to Web version on PubMed Central for supplementary material.

ACKNOWLEDGMENTS

The authors thank Drs. M. Bhuiyan and Q. Ye for their surgical assistance.

SOURCES OF FUNDING

This study was supported by National Institute of Health Grants R01 NS038118 (D.S.) and R01 HL07765 (S.L.A) and R25 (K.K.), and the Manton Center for Orphan Disease Research (K.K.), and a Harvard-MIT Basic Neuroscience Award (K.K.), and the Ministry of Science and Technology, Taiwan (S-S.Y).

REFERENCES

1. Moskowitz MA, Lo EH, Iadecola C. The science of stroke: mechanisms in search of treatments. Neuron. 2010; 67:181–98. [PubMed: 20670828]

2. Muir KW, Lees KR. Clinical experience with excitatory amino acid antagonist drugs. Stroke. 1995; 26:503–13. [PubMed: 7886734]

3. Leng T, Shi Y, Xiong ZG, Sun D. Proton-sensitive cation channels and ion exchangers in ischemic brain injury: new therapeutic targets for stroke? Prog Neurobiol. 2014; 115:189–209. [PubMed: 24467911]

4. Song M, Yu SP. Ionic regulation of cell volume changes and cell death after ischemic stroke. Transl Stroke Res. 2014; 5:17–27. [PubMed: 24323733]

5. Shah NH, Aizenman E. Voltage-gated potassium channels at the crossroads of neuronal function, ischemic tolerance, and neurodegeneration. Transl Stroke Res. 2014; 5:38–58. [PubMed: 24323720]

6. Simard JM, Kent TA, Chen M, Tarasov KV, Gerzanich V. Brain oedema in focal ischaemia: molecular pathophysiology and theoretical implications. Lancet Neurol. 2007; 6:258–68. [PubMed: 17303532]

7. Yan Y, Dempsey RJ, Flemmer A, Forbush B, Sun D. Inhibition of Na(+)-K(+)-Cl(−) cotransporter during focal cerebral ischemia decreases edema and neuronal damage. Brain Res. 2003; 961:22–31. [PubMed: 12535773]

8. Chen H, Luo J, Kintner DB, Shull GE, Sun D. Na^+-dependent chloride transporter (NKCC1)-null mice exhibit less gray and white matter damage after focal cerebral ischemia. J Cereb Blood Flow Metab. 2005; 25:54–66. [PubMed: 15678112]

9. Huang CL, Cha SK, Wang HR, Xie J, Cobb MH. WNKs: protein kinases with a unique kinase domain. Exp Mol Med. 2007; 39:565–73. [PubMed: 18059132]

10. Kahle KT, Ring AM, Lifton RP. Molecular physiology of the WNK kinases. Annu Rev Physiol. 2008; 70:329–55. [PubMed: 17961084]

11. Gagnon KB, Delpire E. Molecular physiology of SPAK and OSR1: two Ste20-related protein kinases regulating ion transport. Physiol Rev. 2012; 92:1577–617. [PubMed: 23073627]

12. Alessi DR, Zhang J, Khanna A, Hochdorfer T, Shang Y, Kahle KT. The WNK-SPAK/OSR1 pathway: Master regulator of cation-chloride cotransporters. Sci Signal. 2014; 7:re3. [PubMed: 25028718]

13. Piala AT, Moon TM, Akella R, He H, Cobb MH, Goldsmith EJ. Chloride sensing by WNK1 involves inhibition of autophosphorylation. Sci Signal. 2014; 7:ra41. [PubMed: 24803536]

14. Deaton SL, Sengupta S, Cobb MH. WNK kinases and blood pressure control. Curr Hypertens Rep. 2009; 11:421–6. [PubMed: 19895753]

15. Kahle KT, Rinehart J, Giebisch G, Gamba G, Hebert SC, Lifton RP. A novel protein kinase signaling pathway essential for blood pressure regulation in humans. Trends Endocrinol Metab. 2008; 19:91–5. [PubMed: 18280177]

16. Pacheco-Alvarez D, Gamba G. WNK3 is a putative chloride-sensing kinase. Cell Physiol Biochem. 2011; 28:1123–34. [PubMed: 22179001]

17. Kahle KT, Rinehart J, de Los HP, Louvi A, Meade P, Vazquez N, et al. WNK3 modulates transport of Cl- in and out of cells: implications for control of cell volume and neuronal excitability. Proc Natl Acad Sci U S A. 2005; 102:16783–8. [PubMed: 16275911]

18. Holden S, Cox J, Raymond FL. Cloning, genomic organization, alternative splicing and expression analysis of the human gene WNK3 (PRKWNK3). Gene. 2004; 335:109–19. [PubMed: 15194194]

19. Haas BR, Cuddapah VA, Watkins S, Rohn KJ, Dy TE, Sontheimer H. With-No-Lysine Kinase 3 (WNK3) stimulates glioma invasion by regulating cell volume. Am J Physiol Cell Physiol. 2011; 301:C1150–C1160. [PubMed: 21813709]

20. Thastrup JO, Rafiqi FH, Vitari AC, Pozo-Guisado E, Deak M, Mehellou Y, et al. SPAK/OSR1 regulate NKCC1 and WNK activity: analysis of WNK isoform interactions and activation by T-loop trans-autophosphorylation. Biochem J. 2012; 441:325–37. [PubMed: 22032326]

21. de Los HP, Kahle KT, Rinehart J, Bobadilla NA, Vazquez N, San CP, et al. WNK3 bypasses the tonicity requirement for K-Cl cotransporter activation via a phosphatase-dependent pathway. Proc Natl Acad Sci U S A. 2006; 103:1976–81. [PubMed: 16446421]

22. Vitari AC, Thastrup J, Rafiqi FH, Deak M, Morrice NA, Karlsson HK, et al. Functional interactions of the SPAK/OSR1 kinases with their upstream activator WNK1 and downstream substrate NKCC1. Biochem J. 2006; 397:223–31. [PubMed: 16669787]

23. Oi K, Sohara E, Rai T, Misawa M, Chiga M, Alessi DR, et al. A minor role of WNK3 in regulating phosphorylation of renal NKCC2 and NCC co-transporters in vivo. Biol Open. 2012; 1:120–7. [PubMed: 23213404]
24. Mederle K, Mutig K, Paliege A, Carota I, Bachmann S, Castrop H, et al. Loss of WNK3 is compensated for by the WNK1/SPAK axis in the kidney of the mouse. Am J Physiol Renal Physiol. 2013; 304:F1198–F1209. [PubMed: 23427142]
25. Flagella M, Clarke LL, Miller ML, Erway LC, Giannella RA, Andringa A, et al. Mice lacking the basolateral Na-K-2Cl cotransporter have impaired epithelial chloride secretion and are profoundly deaf. J Biol Chem. 1999; 274:26946–55. [PubMed: 10480906]
26. Luo J, Wang Y, Chen H, Kintner DB, Cramer SW, Gerdts JK, et al. A concerted role of Na(+)-K(+)-Cl(−) cotransporter and Na(+)/Ca(2+) exchanger in ischemic damage. J Cereb Blood Flow Metab. 2008; 28:737–46. [PubMed: 17912271]
27. Belayev L, Alonso OF, Busto R, Zhao W, Ginsberg MD. Middle cerebral artery occlusion in the rat by intraluminal suture. Neurological and pathological evaluation of an improved model. Stroke. 1996; 27:1616–22. [PubMed: 8784138]
28. Swanson RA, Morton MT, Tsao-Wu G, Savalos RA, Davidson C, Sharp FR. A semiautomated method for measuring brain infarct volume. J Cereb Blood Flow Metab. 1990; 10:290–3. [PubMed: 1689322]
29. Chen H, Luo J, Kintner DB, Shull GE, Sun D. Na(+)-dependent chloride transporter (NKCC1)-null mice exhibit less gray and white matter damage after focal cerebral ischemia. J Cereb Blood Flow Metab. 2005; 25:54–66. [PubMed: 15678112]
30. Pedraza CE, Monk R, Lei J, Hao Q, Macklin WB. Production, characterization, and efficient transfection of highly pure oligodendrocyte precursor cultures from mouse embryonic neural progenitors. Glia. 2008; 56:1339–52. [PubMed: 18512250]
31. Beck J, Lenart B, Kintner DB, Sun D. Na-K-Cl cotransporter contributes to glutamate-mediated excitotoxicity. J Neurosci. 2003; 23:5061–8. [PubMed: 12832529]
32. Shi Y, Chanana V, Watters JJ, Ferrazzano P, Sun D. Role of sodium/hydrogen exchanger isoform 1 in microglial activation and proinflammatory responses in ischemic brains. J Neurochem. 2011; 119:124–35. [PubMed: 21797866]
33. Zhou J, Zhuang J, Li J, Ooi E, Bloom J, Poon C, et al. Long-term post-stroke changes include myelin loss, specific deficits in sensory and motor behaviors and complex cognitive impairment detected using active place avoidance. PLoS One. 2013; 8:e57503. [PubMed: 23505432]
34. Krueger M, Hartig W, Reichenbach A, Bechmann I, Michalski D. Blood-brain barrier breakdown after embolic stroke in rats occurs without ultrastructural evidence for disrupting tight junctions. PLoS One. 2013; 8:e56419. [PubMed: 23468865]
35. Chen H, Kintner DB, Jones M, Matsuda T, Baba A, Kiedrowski L, et al. AMPA-mediated excitotoxicity in oligodendrocytes: role for Na(+)-K(+)-Cl(−) co-transport and reversal of Na(+)/Ca(2+) exchanger. J Neurochem. 2007; 102:1783–95. [PubMed: 17490438]
36. Moriguchi T, Urushiyama S, Hisamoto N, Iemura S, Uchida S, Natsume T, et al. WNK1 regulates phosphorylation of cation-chloride-coupled cotransporters via the STE20-related kinases, SPAK and OSR1. J Biol Chem. 2005; 280:42685–93. [PubMed: 16263722]
37. Ohta A, Rai T, Yui N, Chiga M, Yang SS, Lin SH, et al. Targeted disruption of the Wnk4 gene decreases phosphorylation of Na-Cl cotransporter, increases Na excretion and lowers blood pressure. Hum Mol Genet. 2009; 18:3978–86. [PubMed: 19633012]
38. Darman RB, Forbush B. A regulatory locus of phosphorylation in the N terminus of the Na-K-Cl cotransporter, NKCC1. J Biol Chem. 2002; 277:37542–50. [PubMed: 12145304]
39. McIver SR, Muccigrosso M, Gonzales ER, Lee JM, Roberts MS, Sands MS, et al. Oligodendrocyte degeneration and recovery after focal cerebral ischemia. Neuroscience. 2010; 169:1364–75. [PubMed: 20621643]
40. Matute C, Domercq M, Perez-Samartin A, Ransom BR. Protecting white matter from stroke injury. Stroke. 2013; 44:1204–11. [PubMed: 23212168]
41. Lee HH, Jurd R, Moss SJ. Tyrosine phosphorylation regulates the membrane trafficking of the potassium chloride co-transporter KCC2. Mol Cell Neurosci. 2010; 45:173–9. [PubMed: 20600929]

42. Hossain Khan MZ, Sohara E, Ohta A, Chiga M, Inoue Y, Isobe K, et al. Phosphorylation of Na-Cl cotransporter by OSR1 and SPAK kinases regulates its ubiquitination. Biochem Biophys Res Commun. 2012; 425:456–61. [PubMed: 22846565]
43. O'Donnell ME, Lam TI, Tran L, Anderson SE. The role of the blood-brain barrier Na-K-2Cl cotransporter in stroke. Adv Exp Med Biol. 2004; 559:67–75. [PubMed: 18727228]
44. Chen H, Kintner DB, Jones M, Matsuda T, Baba A, Kiedrowski L, et al. AMPA-mediated excitotoxicity in oligodendrocytes: role for Na(+)-K(+)-Cl(−) co-transport and reversal of Na(+)/Ca(2+) exchanger. J Neurochem. 2007; 102:1783–95. [PubMed: 17490438]
45. Chen X, Kintner DB, Baba A, Matsuda T, Shull GE, Sun D. Protein aggregation in neurons following OGD: a role for Na+ and Ca2+ ionic dysregulation. J Neurochem. 2010; 112:173–82. [PubMed: 19840218]
46. Chen X, Kintner DB, Luo J, Baba A, Matsuda T, Sun D. Endoplasmic reticulum Ca2+ dysregulation and endoplasmic reticulum stress following in vitro neuronal ischemia: role of Na+-K+-Cl- cotransporter. J Neurochem. 2008; 106:1563–76. [PubMed: 18507737]
47. Dmytrenko L, Cicanic M, Anderova M, Vorisek I, Ottersen OP, Sykova E, et al. The impact of alpha-syntrophin deletion on the changes in tissue structure and extracellular diffusion associated with cell swelling under physiological and pathological conditions. PLoS One. 2013; 8:e68044. [PubMed: 23861848]
48. Matsuoka Y, Hossmann KA. Cortical impedance and extracellular volume changes following middle cerebral artery occlusion in cats. J Cereb Blood Flow Metab. 1982; 2:466–74. [PubMed: 7142310]
49. Hansen AJ, Zeuthen T. Extracellular ion concentrations during spreading depression and ischemia in the rat brain cortex. Acta Physiol Scand. 1981; 113:437–45. [PubMed: 7348028]
50. Yan Y, Merlin D. Ste20-related proline/alanine-rich kinase: a novel regulator of intestinal inflammation. World J Gastroenterol. 2008; 14:6115–21. [PubMed: 18985800]
51. Jayakumar AR, Liu M, Moriyama M, Ramakrishnan R, Forbush B III, Reddy PV, et al. Na-K-Cl Cotransporter-1 in the mechanism of ammonia-induced astrocyte swelling. J Biol Chem. 2008; 283:33874–82. [PubMed: 18849345]
52. Schomberg SL, Su G, Haworth RA, Sun D. Stimulation of Na-K-2Cl cotransporter in neurons by activation of Non-NMDA ionotropic receptor and group-I mGluRs. J Neurophysiol. 2001; 85:2563–75. [PubMed: 11387401]
53. Sun D, Murali SG. Stimulation of Na+-K+-2Cl- cotransporter in neuronal cells by excitatory neurotransmitter glutamate. Am J Physiol. 1998; 275:C772–C779. [PubMed: 9730961]
54. Gagnon KB, Delpire E. Physiology of SLC12 transporters: lessons from inherited human genetic mutations and genetically engineered mouse knockouts. Am J Physiol Cell Physiol. 2013; 304:C693–C714. [PubMed: 23325410]
55. Sengupta S, Tu SW, Wedin K, Earnest S, Stippec S, Luby-Phelps K, et al. Interactions with WNK (with no lysine) family members regulate oxidative stress response 1 and ion co-transporter activity. J Biol Chem. 2012; 287:37868–79. [PubMed: 22989884]
56. Lee AY, Chen W, Stippec S, Self J, Yang F, Ding X, et al. Protein kinase WNK3 regulates the neuronal splicing factor Fox-1. Proc Natl Acad Sci U S A. 2012; 109:16841–6. [PubMed: 23027929]

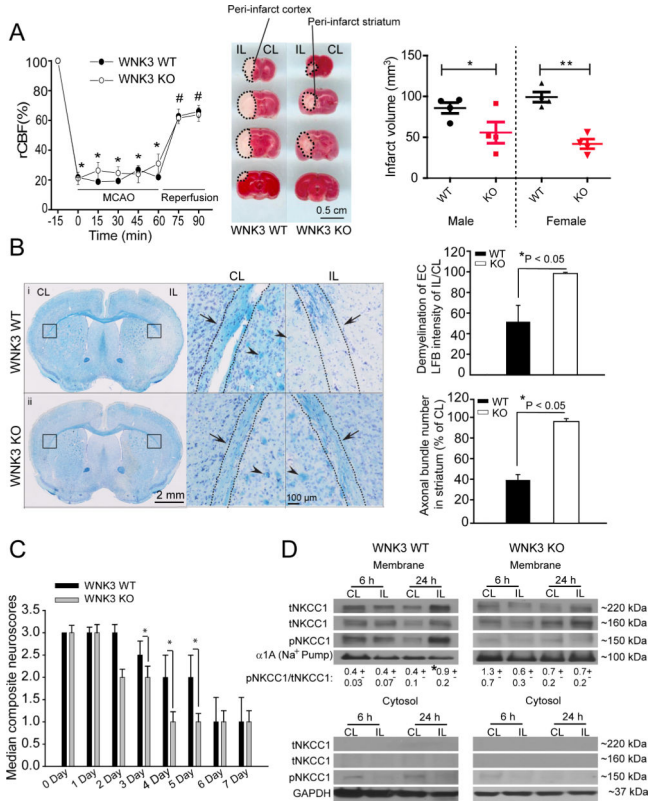

Figure 1. Genetic deletion of *WNK3 in vivo* decreases infarct volume and demyelination and improves neurological recovery following ischemic stroke

A. Changes in regional cerebral blood flow (rCBF) during and after 60-min MCAO are similar in littermate wild type (WT) and *WNK3* KO mice. Values are mean ± SD. *p < 0.05 *vs.* -15 min, #p < 0.05 vs 0 min with one-way ANOVA . Representative coronal brain sections from WT and *WNK3* KO mice. Infarct volume at 24 h Rp was determined by TTC staining. Values are mean ± SEM (n = 8, 4F/4M). *p < 0.05 *vs.* WT. **B.** *WNK3* KO mice exhibit less white matter injury after MCAO than WT. Left panel: Bright field images of WT (i) or *WNK3* KO brain sections (ii) stained with Luxol Fast Blue (LFB) and cresyl violet. *Black box*: Demyelination analysis in external capsules (EC) of white matter in the CL and IL hemispheres. Right panel: higher magnification images. *Arrowhead*: myelinated or demyelinated axonal bundles. *Arrow*: Axonal track. **Right panel**, Summary of demyelination data. Values are Mean ± SEM (n = 3). *p < 0.05 *vs.* WT. **C.** Improved neurological behavior in *WNK3* KO mice after MCAO, scored as described in Methods [27]. Values are median composite values and data analyzed by non-parametric Mann-Whitney test (n= 8-9, M). *p < 0.05 *vs.* WT, #p < 0.05 *vs.* 0 day. **D**. Expression of pNKCC1 in cytosolic or membrane fractions of ischemic brains. Values are Mean ± SEM (n= 3-4). *p < 0.05 *vs.* CL.

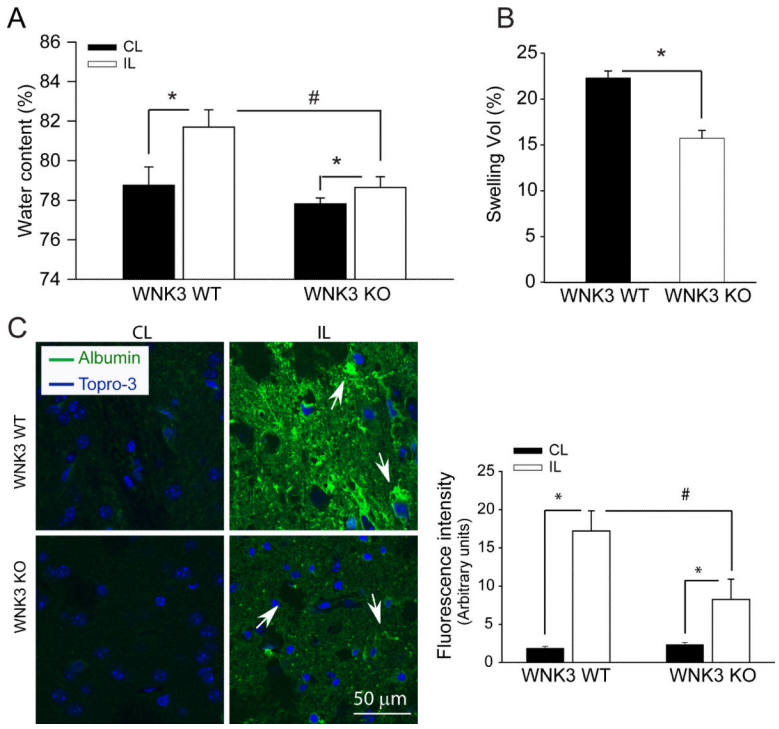

Figure 2. WNK3 KO mice exhibited less edema and BBB leakage after focal ischemia

A-B. Brain water content and percentage of hemispheric swelling at 24 h after MCAO. Values are expressed as mean ± SD (n = 4-8). *P < 0.05. C. Representative albumin immnunofluorescence staining in the striatum of WNK3 WT and WNK3 KO brain sections (arrows). Right panel, summary of albumin infiltration. Albumin immunoreactivity was quantified by measuring the fluorescence intensity of images in panel C. At least three independent areas were quantified from each mouse brain. Values are expressed as mean ± SEM (n = 5), *P < 0.05.

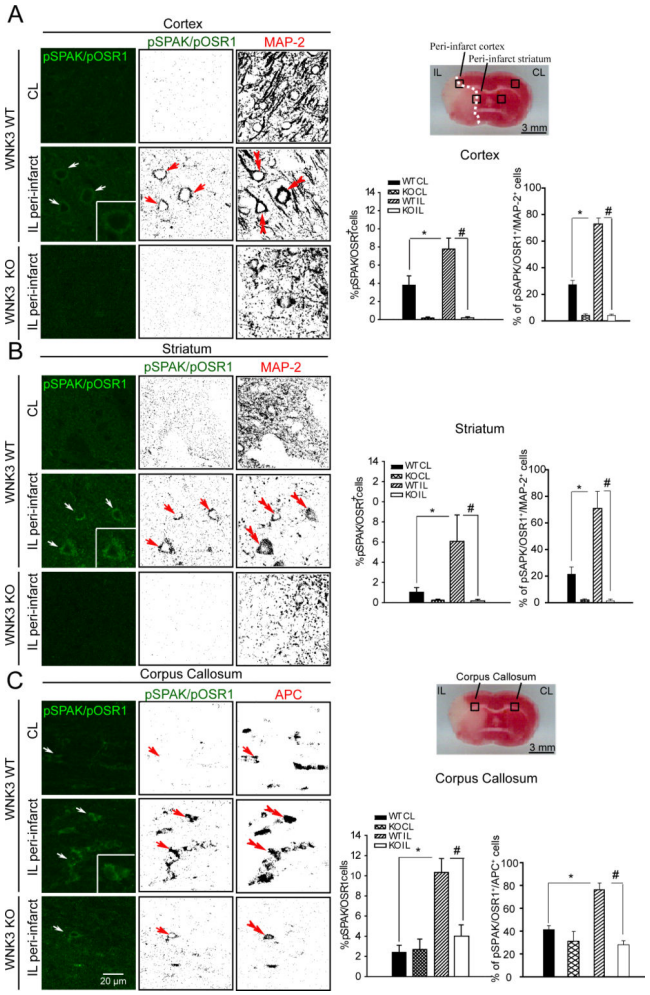

Figure 3. Focal ischemia triggers the activating phosphorylation of the WNK3 kinase substrates SPAK/OSR1 kinase in neurons and oligodendrocytes

A-C. Representative images and binary images of pSPAK/pOSR1 (*green*), the neuronal marker MAP-2, or the mature oligodendrocyte marker APC staining in cortex (A), striatum (B) or corpus callosum (C) in the CL and IL of *WNK3* WT or *WNK3* KO mice were shown after MCAO. *Arrow:* neurons or oligodendrocytes with increased expression of pSPAK/pOSR1. *Double arrowhead*: $MAP2^+$ neurons. *Scale bar*: 20 μm. **Right panels**, Illustration of the ischemic core and peri-infarct tissue (i.e., penumbra), and sample collections from peri-infarct areas (black box) at 6 h Rp following MCAO. Summary of pSPAK/pOSR1 expression data in total cells (TO-PRO-3-positive cells) or in neurons (MAP-2-positive cells). Illustration of a representative peri-infarct area of corpus callosum (black box) at 3 d Rp following MCAO. Summary of pSPAK/OSR1 expression in total cells (TO-PRO-3-positive cells) or oligodendrocytes (APC-positive cells). Values represent mean ± S.E.M. (n = 3), *P < 0.05. # P < 0.05.

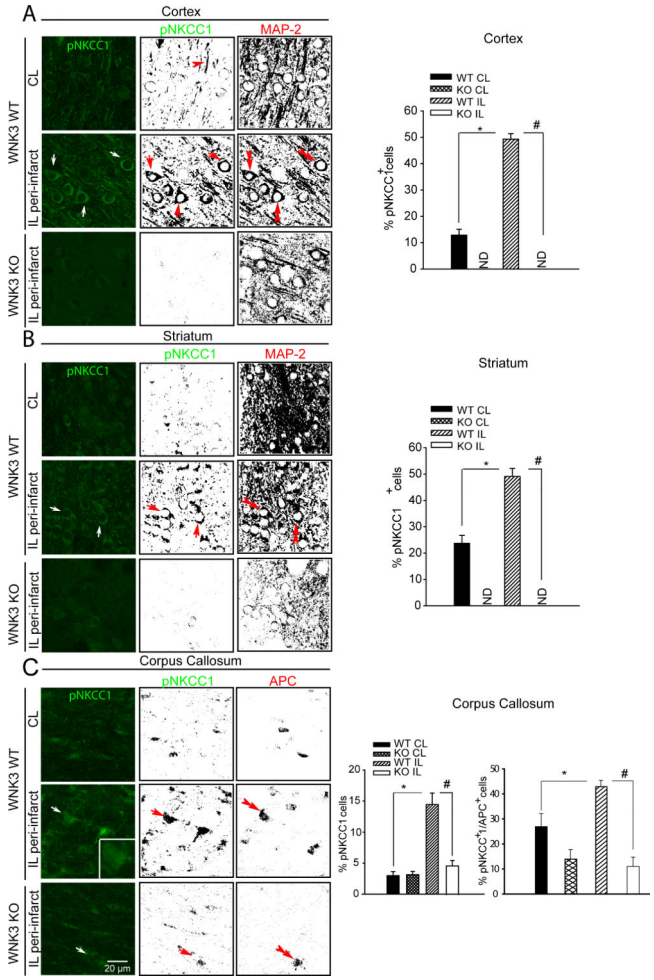

Figure 4. WNK3-dependent phospho-activation of the NKCC1 cotransporter in ischemic neurons and oligodendrocytes *in vivo*

A and B. Representative immunofluorescence images and binary images of pNKCC1 (*green*) and MAP-2 *(red)* staining in WT or *WNK3* KO mouse cortex (A) or striatum (B) after 24 h Rp following MCAO. *Arrow*: neurons or oligodendrocytes with increased functional expression of pNKCC1.*Double arrowhead*: $MAP2^+$ neurons. *Scale bar*: 20 μm. **C**. Representative images of pNKCC1 (*green*) or APC (*red*) staining in the corpus callosum after 3 d Rp following MCAO. Right panels, Summary pNKCC1 expression data in total cells (TO-PRO-3-positive cells). Values represent mean ± S.E.M (n = 3). * p <0.05 vs. CL. Summary of pNKCC1 expression data in mature oligodendrocytes (APC-positive cells). Values represent mean ± S.E.M. (n = 4). *P < 0.05. # P < 0.05.

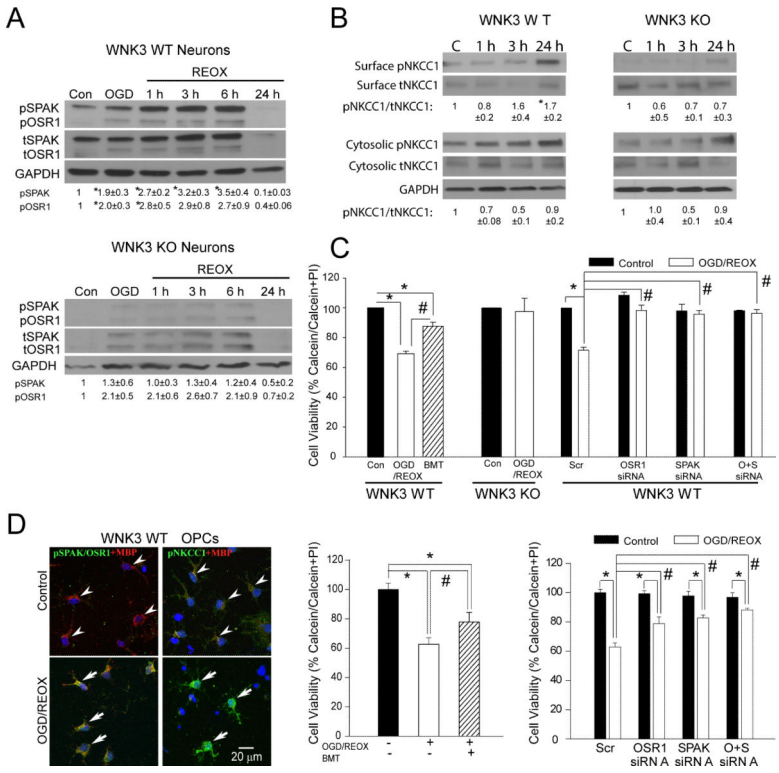

Figure 5. Knockout of WNK3 or SPAK/OSR1 protects neurons and OPCs against ischemic damage

A. Representative immunoblot of pSPAK and pOSR1 expression in primary cortical neurons of WT or WNK3 KO mice after 2 h oxygen-and-glucose deprivation (OGD) or after subsequent reoxygenation (REOX) for durations of 1, 3, 6 or 24 h. **B**. Neuronal expression of pNKCC1 in cytosolic fraction or at the cell surface membrane as detected by surface biotinylation (see Supplemental Methods). Values represent Mean ± SEM (n = 3-5). **C**. Summary of neuronal viability data under control or Scrambled (Scr) control conditions, OGD/REOX plus bumetanide (BMT; 10 μM for 24 h), or treated with SPAK and OSR1 siRNAs. Data are normalized to the scrambled group. Values represent Mean ± S.E.M. (n = 3). *P <0.05. # P < 0.05. **D**. Elevated expression of pSPAK/OSR1 and pNKCC1 in MBP-positive OPCs after OGD/REOX. Right panels, OPC survival after OGD/REOX with NKCC1 inhibition by BMT. Knockdown of *SPAK/OSR1* by siRNA increases viability of OPC. Values represent Mean ± S.E.M. (n = 3-5). *P < 0.05. # P < 0.05.